# Modified Newtonian dynamics habitats within the solar system

Jacob Bekenstein[1] and João Magueijo[2,3,4]

[1]*Racah Institute of Physics, Hebrew University of Jerusalem, Jerusalem 91904, Israel*
[2]*Perimeter Institute for Theoretical Physics, 31 Caroline St. N., Waterloo, N2L 2Y5, Canada*
[3]*Canadian Institute for Theoretical Astrophysics, 60 St. George St., Toronto, M5S 3H8, Canada*
[4]*Theoretical Physics Group, Imperial College, Prince Consort Road, London SW7 2BZ, United Kingdom*

MOdified Newtonian Dynamics (MOND) is an interesting alternative to the presence of dark matter in galaxies. We here examine the possibility that mild or even strong MOND behavior may become evident well inside the solar system, in particular, near saddle points of the total gravitational potential. Whereas in Newtonian theory tidal stresses are finite at saddle points, they are expected to diverge in MOND, and to remain distinctly large inside a sizable oblate ellipsoid around the saddle point. We work out the MOND effects using the nonrelativistic limit of the T$e$V$e$S theory, both in the perturbative nearly Newtonian regime and in the deep MOND regime. While strong MOND behavior would be a spectacular "backyard" vindication of the theory, pinpointing the MOND bubbles in the setting of the realistic solar system may be difficult. Space missions, such as the LISA Pathfinder, equipped with sensitive accelerometers, may be able to explore the larger perturbative region.

## I. INTRODUCTION

MOND [1] is a scheme for explaining observed regularities and correlations in the dynamical properties of galaxies without invoking dark matter. It has been very successful in this job despite its rather rudimentary form [2]. In the Lagrangian formulation of MOND [3] the physical gravitational potential $\Phi$, which gives test particle acceleration by $\mathbf{a} = -\nabla\Phi$, is determined by the modified Poisson equation

$$\nabla \cdot [\tilde{\mu}(|\nabla\Phi|/a_0)\nabla\Phi] = 4\pi G\tilde{\rho}, \qquad (1)$$

where $\tilde{\rho}$ is the baryonic mass density, $a_0 \approx 10^{-10} \text{ m s}^{-2}$ is Milgrom's characteristic acceleration, and the function $\tilde{\mu}(x)$ is required to approximate its argument for $x \ll 1$ and to approach unity for $x \gg 1$. The form

$$\tilde{\mu}(x) = x(1 + x)^{-1} \qquad (2)$$

has been quite successful in modelling galaxy rotation curves without invoking dark matter. The theory encapsulated in Eq. (1) has recently been reformulated as a consistent covariant gravitation theory named T$e$V$e$S [4]. Alternatives to this theory have been considered [5–7], but they shall not be employed in the present work.

Are MOND effects of importance in the solar system (henceforth SS)? Milgrom was the first to consider the effects of MOND on the properties of long period comets originating in the Oort cloud [1]. It was later observed that relativistic theories with a MOND limit can easily predict anomalously large perihelion precessions of the planets [6,8]. With the discovery of the "Pioneer anomaly" [9] much speculation was directed towards a possible MONDian origin of the effect [10]. Relativistic theories with MOND phenomenology tend to produce a radial drift of the Kepler constant in the SS in the same sense as would

correspond to the claimed Pioneer effect, though not always of the claimed magnitude [2,4,6,11]. The persistence of Pioneer-type effects in a variety of scalar-tensor theories of MOND, and the hurdles faced by such theories from precision SS tests has been emphasized by Sanders [6].

In this paper we search for other sites deep inside the SS where strong MOND behavior might put the MOND phenomenon at the reach of spacecraft measurements. Strong MOND behavior is triggered by a low gradient in the *total* Newtonian potential $\Phi_N$ (the deep MOND regime is that where $|\nabla\Phi| \ll a_0$). Two apparent candidates for strong MOND regions fail this criterion. Most obviously we have gravitational perturbations, such as those accounting for the nonrelativistic component of the perihelion of Mercury precession, or Neptune's influence upon Uranus' orbit. Most of these have a very low potential gradient, and would by themselves be in the MOND regime. However the gradient of the total $\Phi_N$ is not small, so their effect falls in the Newtonian regime. Issues like the stability of the SS or its detailed dynamics are not expected to be appreciably different in MOND.

The Lagrange points are another apparent possibility for strong MOND regions. They are the five stationary points of the two-body dynamics; for example, L1 is the point between the Earth and the Sun where a test mass would be in inertial motion, moving neither towards the Sun nor the Earth. Each Lagrangian point orbits the Sun with the same frequency as the Earth, so the gradient of $\Phi_N$ at it must cancel the corresponding centrifugal acceleration, and is thus not especially small. This does not mean, as we shall see, that perturbative effects around these points are not present; however strong MONDian behavior is certainly not expected.

By contrast, the saddle (or extremum) point (henceforth SP) of $\Phi_N$ between two gravitating bodies is evidently in

103513-1

the deep MOND regime, since $\nabla \Phi_N = 0$ there. One such point exists between any two gravitating bodies, potentially providing a testing ground for strong MONDian behavior. SPs are not inertial, but may be visited by free-falling test bodies; they are encased by small "bubbles" within which strong MOND effects are expected.

In what follows we study the structure of the gravitational field in increasingly smaller neighborhoods of the SP for a binary mass system. Principally we look at the encasing Newtonian region, at the enclosed quasi-Newtonian sector and at the deep MOND region at the heart of the bubble. The strongly nonlinear character of the MOND phenomenon makes the analysis complicated, and a variety of analytical as well as numerical strategies have been utilized.

The plan of this paper is as follows. In Sec. II we lay down the framework for dealing with the two (and many) body problem in MOND. In Sec. III we use heuristic arguments to find the location and extent of the principal MOND bubble for a binary system. One of the approximations thus made is replaced by a more exact treatment in Sec. IV. In Sec. V we perturbatively calculate the gravitational field in the quasi-Newtonian region still far from the SP point. In Sec. VI a combination of numerical and analytical approaches is used to deduce the gravitational field very near the SP where MOND is dominant. In Sec. VII we discuss a number of complications to the above stylized treatment that arise from the many-body nature of the real SS. The prospect of a direct test using the LISA Pathfinder project [12] is briefly discussed in Sec. VIII. Issues connected with the behavior of gravity in the spacecraft's frame are elucidated in the appendix. We conclude in Sec. IX with a statement on how our work might help settling the controversy between dark matter and MOND.

## II. THE FRAMEWORK OF THE MANY-BODY PROBLEM

Where needed we use units with $c = 1$. We base the analysis on the nonrelativistic limit of T$e$V$e$S [4]; AQUAL [3] and other Lagrangian formulations of MOND have similar form and many of our conclusions may apply to all of them. In T$e$V$e$S the MOND behavior is driven by a dynamical (and dimensionless) scalar field $\phi$ such that the physical potential $\Phi$ in which a body falls is given by $\Phi = \Phi_N + \phi$, where $\Phi_N$ is the usual Newtonian potential (inferred from the metric component $g_{00}$). In the nonrelativistic regime $\phi$ is governed by the equation

$$\nabla \cdot [\mu(kl^2(\nabla \phi)^2)\nabla \phi] = kG\tilde{\rho}, \qquad (3)$$

where $k$ is a coupling constant and $l$ is a length scale which determines the Milgrom acceleration by

$$a_0 = \frac{\sqrt{3k}}{4\pi l} \approx 10^{-10} \text{ m s}^{-2} \qquad (4)$$

(we are setting $\Xi$, as defined in [4], to unity; thus we ignore the slight renormalization of the gravitational constant in T$e$V$e$S so that here $G_N = G$). In Eq. (3) $\mu$ is a free function not to be confused with Milgrom's $\tilde{\mu}$. Reference [4] proposed a particular form for it. The deep MOND regime is signalled by the low gradient of the scalar field $\phi$; in this regime

$$\mu \approx \frac{k}{4\pi} \frac{|\nabla \phi|}{a_0}. \qquad (5)$$

For strong gradients the $\mu$ proposed in Ref. [4] grows crudely as $(|\nabla \phi|/a_0)^{2/3}$. This has the effect of suppressing the contribution of $\nabla \phi$ to $\nabla \Phi$ thus bringing in the Newtonian regime. In spherically symmetric systems T$e$V$e$S with any $\mu$ satisfying Eq. (5) goes over into the Lagrangian MOND theory (1) with Milgrom's $\tilde{\mu}$ given by $\tilde{\mu} = (1 + k/4\pi\mu)^{-1}$. Although this point is not well explored, it is quite possible that in less symmetric systems T$e$V$e$S does not go over to an exactly MOND behavior. For this reason we base this paper on the nonrelativistic limit of T$e$V$e$S, and not on Lagrangian MOND.

We need to solve Eq. (3) for a many-body source, but that equation is nonlinear so the $\phi$ fields due to each body do not superpose. However any nonlinear equation may be *formally* linearized by an appropriate change of variables. Here this is

$$\mathbf{u} = -\frac{4\pi\mu}{k}\nabla \phi \qquad (6)$$

(see [13], where this technique was first suggested). We may then add the $\mathbf{u}$ due to each source (which is the Newtonian acceleration) and invert the *total* $\mathbf{u}$ at a given point to find $\nabla \phi$. It is essential that the sum of all sources be performed before inverting to find $\nabla \phi$.

This algorithm may be applied to any number of components. But note that even if a term in the sum is in the MOND regime, the overall system is not, unless the total $|\mathbf{u}|$ is much smaller than $a_0$. (It is because of this feature that the gravitational perturbations in the SS are non-MONDian.) However, it is also possible to have two components with fields not in the MOND regime such that their common field is MONDian in some region. Examples are the SPs in the gravitational potential of two bodies to be studied in this paper.

The only complication with the above technique is that $\mathbf{u}$ is generally not curl-free; indeed it is rather the vector $\mathbf{u}/\mu$ which is curl-free. Thus the full set of equations for $\mathbf{u}$ are

$$\nabla \cdot \mathbf{u} = -4\pi G\tilde{\rho}, \qquad (7)$$

$$\nabla \wedge \frac{\mathbf{u}}{\mu} = 0. \qquad (8)$$

The first equation tells us that $\mathbf{u}$ equals the Newtonian acceleration $\mathbf{F}^{(N)} = -\nabla \Phi_N$ up to a curl, that is, there

must exist a vector field $\mathbf{h}$ such that

$$\mathbf{u} = \mathbf{F}^{(N)} + \nabla \wedge \mathbf{h}. \qquad (9)$$

The second equation fixes the $\mathbf{h}$ (up to a gradient). This operation can only be performed upon the total $\mathbf{u}$, once again stressing the intrinsic nonlinearity of the theory. It can be shown that the curl term vanishes in a spherically symmetric situation, or in the quasi-Newtonian regime far away from the source [3,4]. Near the SPs neither of these conditions is satisfied and we have to evaluate $\nabla \wedge \mathbf{h}$. However, before plunging into the full problem, let us provide some orientation

### III. HEURISTICS OF THE MOND BUBBLES

We now examine the MONDian saddle region under two simplifying assumptions. One is to replace what is essentially a many-body situation (the Solar system) by a two-body problem; the other is to drop the curl term in (9). We warn the reader that these approximations have very different fates. The former escapes largely unscathed from a proper treatment (see Sec. VII), and a two-body calculation can be easily adapted to the full-blown situation. The latter is extremely crude and the curl term evaluated in Secs. IV, V, VI, and VII introduces striking novelties. We present the simplified argument as a benchmark, justifying the rather laborious analysis in Secs. IV, V, VI, and VII.

Consider two bodies at distance $R$ with masses $M$ and $m$, with $M \gg m$, so that the system's center of mass may be taken to coincide with the heavier body. To be definite we call them the Sun and the Earth, but we shall explore other couples later. Along the line linking them (the $z$ axis), the Newtonian acceleration is

$$\mathbf{F}^{(N)} = \left( -\frac{GM}{\tilde{r}^2} + \frac{Gm}{(R - \tilde{r})^2} \right) \mathbf{e}_z, \qquad (10)$$

where $\tilde{r}$ is the distance from the Sun and $\mathbf{e}_z$ is the unit vector in the direction Sun to Earth. The SP of the Newtonian potential $\Phi_N$ resides where $\mathbf{F}^{(N)} = 0$, i.e. at

$$\tilde{r} = r_s \approx R\left( 1 - \sqrt{\frac{m}{M}} \right). \qquad (11)$$

Around this point $\mathbf{F}^{(N)}$ increases linearly as it passes through zero, that is

$$\mathbf{F}^{(N)} \approx A(\tilde{r} - r_s)\mathbf{e}_z, \qquad (12)$$

where

$$A = 2\frac{GM}{r_s^3}\left( 1 + \sqrt{\frac{M}{m}} \right) \qquad (13)$$

is the tidal stress at the SP along the Sun-Earth direction. The full tidal stress matrix is easy to compute. Let us use cylindrical coordinates centered at the SP, with the $z$-axis pointing along the Sun-Earth direction, so that we have

$\partial F_z^{(N)}/\partial z = A$ and $\partial F_\varrho^{(N)}/\partial z = 0$. From the further condition that the divergence must be zero (outside the Sun and Earth) we have

$$\mathbf{F}^{(N)} = A(z\mathbf{e}_z - \tfrac{1}{2}\varrho\mathbf{e}_\varrho). \qquad (14)$$

The region around the SP is obviously in the deep MOND regime since $|\mathbf{F}^{(N)}| \ll a_0$. Thus regardless of the model adopted for $\mu$, we have just on the basis of Eq. (5) that

$$\mathbf{u} \approx -\frac{|\nabla\phi|}{a_0}\nabla\phi = \mathbf{F}^{(N)} + \nabla \wedge \mathbf{h}. \qquad (15)$$

*If we ignore the curl term* and use $|\nabla\phi| \ll |\mathbf{F}^{(N)}|$, we have

$$\mathbf{F} = -\nabla\Phi \approx -\nabla\phi = \sqrt{Aa_0}\frac{z\mathbf{e}_z - \frac{\varrho}{2}\mathbf{e}_\varrho}{(z^2 + \frac{\varrho^2}{4})^{1/4}}, \qquad (16)$$

and we see that in contrast to the Newtonian theory, the tidal stresses here diverge at the SP. This feature survives the introduction of the less intuitive curl term and may be heuristically understood by applying the rule of thumb that in the deep MOND regime the square root of the Newtonian acceleration gives the physical acceleration. According to Eq. (12) Newtonian acceleration increases linearly along the line Sun-Earth, so the physical acceleration in the deep MOND regime is of the form $\pm\sqrt{Aa_0|\tilde{r} - r_s|}$, which has infinite derivative at $r_s$.

What is the size of the region where the tidal stresses remain anomalously high? Naively one might expect that the deep MOND regime is defined by the oblate ellipsoidal region defined by $|\mathbf{F}^{(N)}| = a_0$, which translates into a major semiaxis (in the $\varrho$ direction) of size

$$\delta\tilde{r} = \frac{2a_0}{A} \approx \frac{a_0}{a_m}\sqrt{\frac{m}{M}}R, \qquad (17)$$

where $a_m$ is the acceleration of the smaller mass $m$. This expectation turns out wrong when, in Secs. V and VI, we bring the curl term into play. It is easier to estimate the size of the (larger) region where there are significant perturbative corrections to Newtonian theory, but where deep MOND behavior is not yet in evidence. For the model introduced in [4] Milgrom's $\tilde{\mu}$ can be estimated in the quasi-Newtonian region through formula (69) there (which formula, however, is rigorous only in the spherically symmetric case):

$$\tilde{\mu} = \frac{F^{(N)}}{F} \approx \left( 1 - \frac{16\pi^3}{k^3}\frac{a_0^2}{F^2} \right). \qquad (18)$$

Let us take $F \approx F^{(N)}$ and use Eq. (14). We see that departures at the level $10^{-4}$ from Newtonian gravity occur within a semimajor axis of size

$$\Delta\tilde{r} = \frac{800\pi^{3/2}}{k^{3/2}}\frac{a_0}{A}. \qquad (19)$$

Using $k \approx 0.03$ (as suggested in [4]) this is $\Delta \tilde{r} \approx 1$, 900 Km for the Sun-Earth system, $\Delta \tilde{r} \approx 4.7 \times 10^6$ Km for Sun-Jupiter, and $\Delta \tilde{r} \approx 700$ Km for the Moon-Earth. In contrast with (17) these estimates will withstand the closer scrutiny presented in Sec. V.

## IV. ACCOUNTING FOR THE CURL TERM

By carrying out the curl in Eq. (8) we get

$$\nabla \ln\mu \wedge \mathbf{u} - \nabla \wedge \mathbf{u} = 0, \tag{20}$$

while squaring Eq. (6) gives

$$u^2 = (4\pi/k)^2 \mu^2 |\nabla\phi|^2. \tag{21}$$

In TeVeS $\mu = \mu(k|\nabla\phi|/a_0)$; thus $k^4 u^2/a_0{}^2$ is a function of $\mu$ only. Defining the dimensionless quantity

$$\kappa \equiv \partial \ln u^2 / \partial \ln\mu, \tag{22}$$

we get $\nabla \ln\mu = \kappa^{-1}\nabla u^2/u^2$ so that Eq. (20) becomes

$$\kappa u^2 \nabla \wedge \mathbf{u} + \mathbf{u} \wedge \nabla u^2 = 0. \tag{23}$$

In systems with spherical, cylindrical, or planar symmetry, $\mathbf{u}$ is necessarily collinear with $\nabla |\mathbf{u}|^2$. Then $\nabla \wedge \mathbf{u}$ must vanish everywhere (since $\kappa$ would be expected to vanish only at isolated points). This agrees with the findings of Refs. [3,4] that $\mu\nabla\phi$ and $\mu\nabla\Phi$ are both curl-free in such situations. When the spatial symmetry is lower or nonexistent, the second term in Eq. (23) will not generally vanish, and will be of order $|\mathbf{u}|^3/L$ where $L$ denotes the scale on which quantities vary. Thus if in a region $\kappa \gg 1$, we would expect $|\nabla \wedge \mathbf{u}|$ to be much smaller than its expected magnitude $|\mathbf{u}|/L$; this signals the quasi-Newtonian regime where $\mathbf{u}$ is nearly curl-free.

In TeVeS the manner of transition between the deep MOND and Newtonian regimes is dependent upon the form of $\mu$. The form proposed in Ref. [4] is quite difficult to work with in our context. We shall thus replace it by the implicit expression

$$\frac{\mu}{\sqrt{1 - \mu^4}} = \frac{k}{4\pi} \frac{|\nabla\phi|}{a_0}, \tag{24}$$

which satisfies the limit (5). A simple calculation (see Ref. [4]) then shows that Milgrom's $\tilde{\mu}$, defined by Eq. (1), is here given parametrically by

$$\tilde{\mu} = \zeta(1 + \zeta)^{-1}, \tag{25}$$

$$x = \zeta(1 + \zeta)[1 - (k\zeta/4\pi)^4]^{-1/2} \tag{26}$$

which satisfies the MOND requirements that $\tilde{\mu} \to x$ for $x \ll 1$ and $\tilde{\mu} \to 1$ as $x \to \infty$. Figure 1 compares our $\tilde{\mu}$ with the "simple" $\tilde{\mu}$ of Refs. [1,14].

Eliminating $|\nabla\phi|/a_0$ between Eqs. (21) and (24) gives

$$\frac{u^2}{a_0^2} = \frac{256\pi^4}{k^4} \frac{\mu^4}{1 - \mu^4}. \tag{27}$$
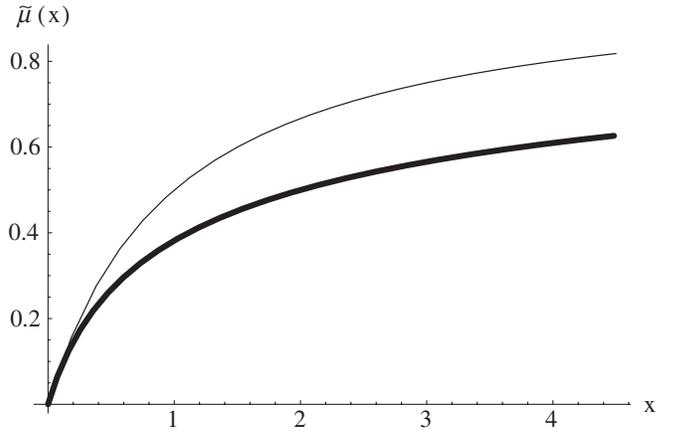


FIG. 1. Milgrom's $\tilde{\mu}$ function (upper curve) as used in many extra-galactic applications (Eq. (2)) and as defined in this paper with $k = 0.03$ by Eqs. (25) and (26).

Differentiating the logarithm of this we calculate that

$$\kappa = \frac{4}{1 - \mu^4} = 4 + \frac{k^4}{64\pi^4} \frac{u^2}{a_0^2}. \tag{28}$$

In terms of the dimensionless vector field

$$\mathbf{U} \equiv \frac{k^2}{16\pi^2} \frac{\mathbf{u}}{a_0} \tag{29}$$

we may thus cast Eqs. (23) and (7) into the form

$$\nabla \cdot \mathbf{U} = 0, \tag{30}$$

$$4(1 + U^2)U^2 \nabla \wedge \mathbf{U} + \mathbf{U} \wedge \nabla U^2 = 0, \tag{31}$$

where we have dropped the source of the first since we are interested only in the region near the SP. This pair of exact equations for one dimensionless vector is central to our study.

Once $\mathbf{U}$ is solved we can recover $\nabla\phi$ by combining Eqs. (6), (27), and (29):

$$-\nabla\phi = \frac{4\pi a_0}{k}(1 + U^2)^{1/4}\frac{\mathbf{U}}{U^{1/2}}. \tag{32}$$

As remarked earlier, the condition $\kappa \gg 1$ brings in the Newtonian limit. Now $\kappa \gg 1$ is equivalent to $U \gg 1$. Obviously in this case $-\nabla\phi \approx (4\pi a_0/k)\mathbf{U} = (k/4\pi)\mathbf{u}$ which tells us by Eq. (6) that $\mu \approx 1$, indeed the Newtonian limit (the same is obvious from Eq. (28)).

## V. THE QUASI-NEWTONIAN REGION

At this point we go over to spherical polar coordinates $(r, \psi, \phi)$ with origin at the SP; accordingly

$$z = r\cos\psi; \qquad \varrho = r\sin\psi. \tag{33}$$

So, for example, Eq. (14) takes the form

$$\mathbf{F}^{(N)} = Ar\mathbf{N}, \tag{34}$$

where

$$\mathbf{N}(\psi) \equiv N_r \mathbf{e}_r + N_\psi \mathbf{e}_\psi, \tag{35}$$

$$N_r = \tfrac{1}{4}[1 + 3\cos(2\psi)], \tag{36}$$

$$N_\psi = -\tfrac{3}{4}\sin(2\psi). \tag{37}$$

We define the quasi-Newtonian region as that where $U^2$ is of order 1 or larger so that the factor $1 + U^2$ cannot be ignored in Eq. (31). The region's size may be estimated by dropping the curl term in (9) (an approximation to be justified *a posteriori*) and finding the solution to $U^2 = 1$ using (14) and (29) (in the Newtonian region $\mathbf{u} = \mathbf{F}^{(N)}$). This leads to the ellipsoid:

$$r^2\left(\cos^2\psi + \frac{1}{4}\sin^2\psi\right) = r_0^2 \equiv \left(\frac{16\pi^2 a_0}{k^2 A}\right)^2. \tag{38}$$

Equation (31) tells us that well outside of this ellipsoid the curl is suppressed by a factor of $1/r^2$ with respect to $\mathbf{F}^{(N)}$. As we show below $\mathbf{U}$ is then neatly separated into a Newtonian component $\mathbf{U}_0$ (carrying the divergence predicted by (7) and depicted in Fig. 2) and a "magnetic" component $\mathbf{U}_2$. By definition $\mathbf{U}_2$ is solenoidal and to leading order is sourced purely by $\mathbf{U}_0$. Specifically the dynamics is approximated by
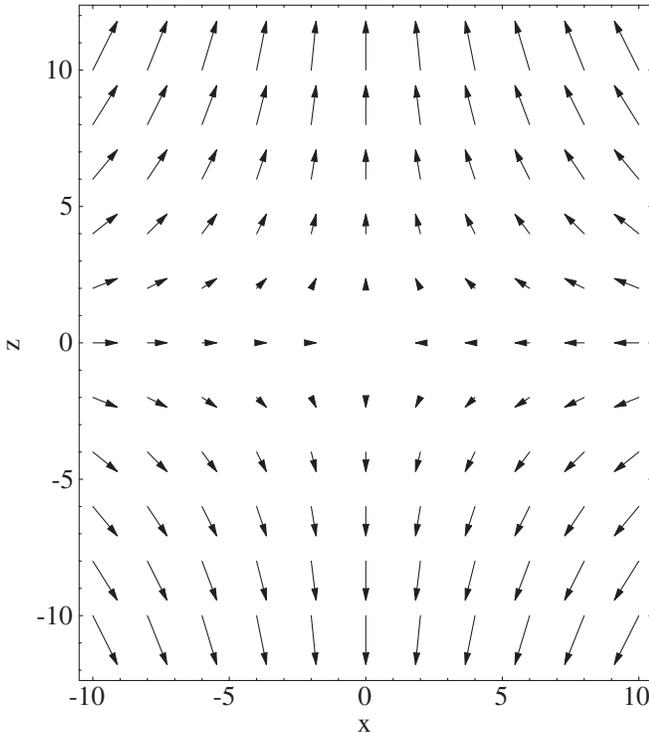
$$\mathbf{U} = \mathbf{U}_0 + \mathbf{U}_2, \tag{39}$$



FIG. 2. The flow of $\mathbf{U}_0$ around the SP (at the origin) in a plane containing the symmetry ($z$) axis; for clarity all vectors have been linearly rescaled.

$$\mathbf{U}_0 = \frac{r}{r_0}\mathbf{N}(\psi), \tag{40}$$

$$\nabla \cdot \mathbf{U}_2 = 0, \tag{41}$$

$$\nabla \wedge \mathbf{U}_2 = -\frac{\mathbf{U}_0 \wedge \nabla|\mathbf{U}_0|^2}{4|\mathbf{U}_0|^4}. \tag{42}$$

With the notation

$$\mathbf{U}_2 = U_r \mathbf{e}_r + U_\psi \mathbf{e}_\psi, \tag{43}$$

Eqs. (41) and (42) become

$$\frac{1}{r^2}\frac{\partial}{\partial r}(r^2 U_r) + \frac{1}{r\sin\psi}\frac{\partial}{\partial\psi}(\sin\psi U_\psi) = 0, \tag{44}$$

$$\frac{1}{r}\left[\frac{\partial}{\partial r}(rU_\psi) - \frac{\partial U_r}{\partial\psi}\right] = \frac{s(\psi)}{r^2}, \tag{45}$$

with

$$s(\psi) \equiv -\frac{3}{8}\frac{\cos\psi\sin\psi}{[\cos^2\psi + \frac{\sin^2\psi}{4}]^2} = -\frac{12\sin2\psi}{(5 + 3\cos2\psi)^2}. \tag{46}$$

The form of Eqs. (44) and (45) suggests that both $U_r$ and $U_\psi$ behave as $1/r$. Accordingly we recast Eq. (43) as the ansatz

$$\mathbf{U}_2 = \frac{r_0}{r}\mathbf{B}(\psi) = \frac{r_0}{r}(F(\psi)\mathbf{e}_r + G(\psi)\mathbf{e}_\psi), \tag{47}$$

where the $r$ dependence has been fully factored out. With this ansatz Eq. (45) collapses into

$$F' = -s = \frac{12\sin2\psi}{(5 + 3\cos2\psi)^2}, \tag{48}$$

with solution

$$F = \frac{2}{5 + 3\cos2\psi} + A, \tag{49}$$

where $A$ is a constant. Equation (44) now becomes

$$F + \frac{1}{\sin\psi}\frac{\partial}{\partial\psi}(\sin\psi G) = 0, \tag{50}$$

which integrates to

$$G\sin\psi = -\int F\sin\psi d\psi + B, \tag{51}$$

where $B$ is another constant. Performing the integral gives

$$G\sin\psi = \frac{\tan^{-1}(\sqrt{3} - 2\tan\frac{\psi}{2}) + \tan^{-1}(\sqrt{3} + 2\tan\frac{\psi}{2})}{\sqrt{3}}$$
$$+ A\cos\psi + B. \tag{52}$$

To determine $A$ and $B$ we must discuss boundary conditions. According to Milgrom [13] for the system (30) and

(31) the normal component of **u** (or **U**) must vanish on all boundaries. Parts of the symmetry axis ($\psi = 0$ as well as $\psi = \pi$) are evidently a boundary of the quasi-Newtonian region; it is obvious that $N_\psi$ vanishes on both North and South parts of it, where it is the normal component. Thus since $\mathbf{U}_0$ satisfies the boundary condition on the relevant pieces of the axis, so must $\mathbf{U}_2$. Accordingly we must require $G(\psi = 0) = G(\psi = \pi) = 0$, from which follows that

$$A = B = -\frac{\pi}{3\sqrt{3}}. \tag{53}$$

The solutions $F$ and $G$ are plotted in Fig. 3. We find that $G(\pi/2) = 0$ as well. Thus on the symmetry plane ($\psi = \pi/2$) **U** is collinear with the axis.

What about the rest of the boundary? We see from Eq. (47) that $\mathbf{U}_2 \to 0$ as $r \to \infty$. Thus at large $r$ our **U** merges with $\mathbf{U}_0$ which we know to be the limiting form of the Newtonian field as we approach the SP. It follows that our solution automatically fulfills the boundary conditions at large $r$. The inward part of the boundary of the quasi-Newtonian region adjoins the intermediate MOND region, where MOND effects are no longer small. Fortunately there is no need for us to set boundary conditions there; rather, the solution just described serves to set boundary conditions for the intermediate MOND region.

We conclude that a SP far away from the strong MOND bubble is characterized by a Newtonian component proportional to $r$ together with a magneticlike perturbation that falls off like $1/r$. The full physical effects in this regime may be appreciated by combining (32) with (40) and (47). We find that the extra acceleration felt by test particles is

$$\delta \mathbf{F} = -\nabla \phi \approx \frac{4\pi a_0}{k} \left( \mathbf{U}_0 + \frac{\mathbf{U}_0}{4U_0^2} + \mathbf{U}_2 + \cdots \right). \tag{54}$$

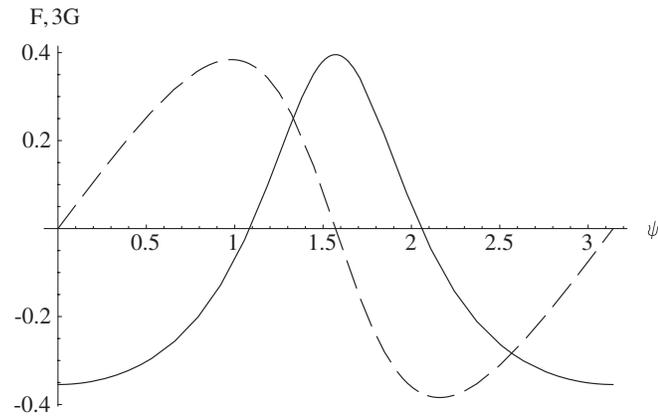The first contribution, call it $\delta \mathbf{F}_0$ is of fully Newtonian form, and just serves to renormalize the gravitational constant, as discussed in [4]. The second term was also derived in [4] (c.f. Eq. (69) of [4]) and is

$$\delta \mathbf{F}_1 = \frac{16\pi^3}{k^3} \frac{a_0^2}{F^{(N)2}} \mathbf{F}^{(N)} = \frac{8\pi a_0}{k} \frac{r_0}{r} \frac{\mathbf{N}(\psi)}{5 + 3\cos(2\psi)}. \tag{55}$$

What we have just shown is that to these two terms one should add the magneticlike contribution

$$\delta \mathbf{F}_2 = \frac{4\pi a_0}{k} \frac{r_0}{r} \mathbf{B}(\psi), \tag{56}$$

which is of the same order of magnitude as $\delta \mathbf{F}_1$. Apart from the prefactor $4\pi a_0/k$, this term is just what was plotted in Fig. 4. In Fig. 5 we plot the angular profile $\mathbf{B}(\psi) + 2[5 + 3\cos(2\psi)]^{-1}\mathbf{N}(\psi)$ of the total correction to the acceleration after renormalization of $G$. The plotted field is to be divided by $r$ (and multiplied by $4\pi a_0 r_0/k$) to obtain the extra acceleration felt by test particles in the quasi-Newtonian region.

How do these results affect the naive expectations of Sec. III? We have just shown that a full quantitative analysis can never neglect the magnetic field derived in this section. In addition the border between full and linear MONDian behavior is determined by the condition $U^2 = 1$, equivalent to ellipsoid (38). As long as we stay well outside this ellipsoid we obtain results consistent with (18) and (19); however the order of magnitude of linear corrections outside this ellipsoid may be written

$$\frac{\delta F}{F^{(N)}} \sim \left( \frac{4\pi}{k} \right)^3 \left( \frac{a_0}{A} \right)^2 \frac{1}{r^2} = \frac{k}{4\pi} \left( \frac{r_0}{r} \right)^2. \tag{57}$$

F, 3G

FIG. 3. The angular profile functions $F$ (solid line) and $G$ (dashed line) giving the direction of the magnetic field **B** in the quasi-Newtonian region; for clarity $G$ has been multiplied by 3.
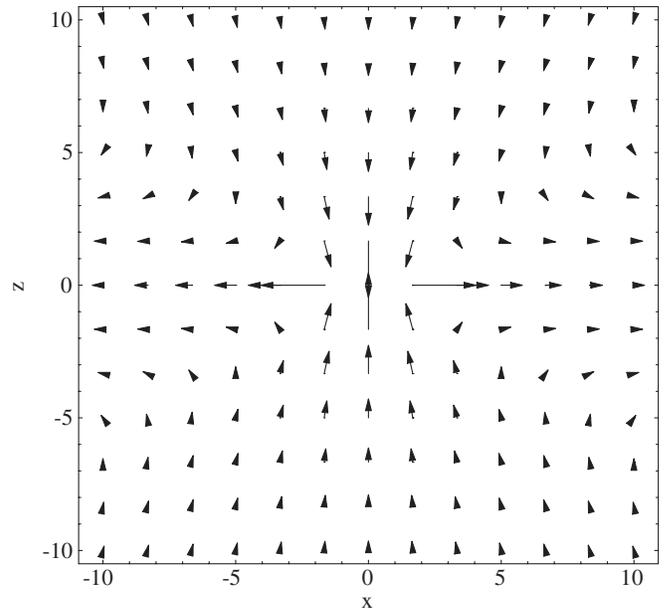
FIG. 4. The flow of $\mathbf{U}_2$ in a plane containing the $z$ axis; coordinates are in units of $r_0$. For clarity the solution was cut off at $r = r_0$ (so as to avoid a divergence at the origin).
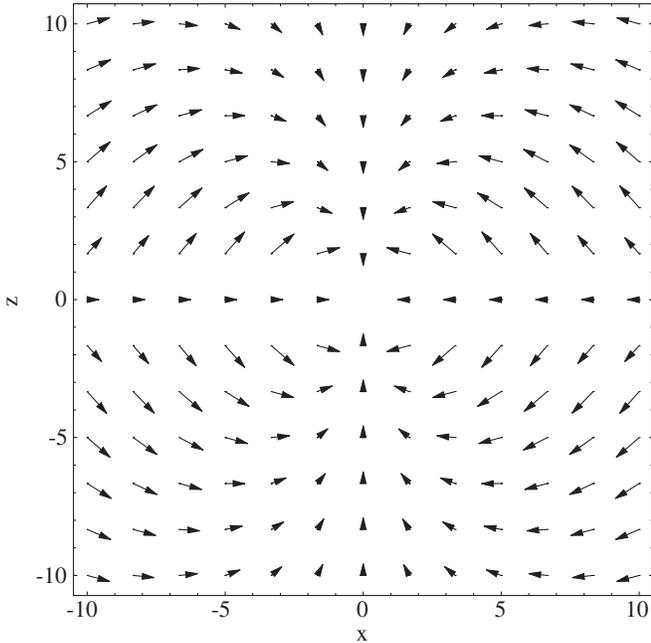
FIG. 5. The flow of $\mathbf{B}(\psi) + 2[5 + 3\cos(2\psi)]^{-1}\mathbf{N}(\psi)$. When divided by $r$ and multiplied by $4\pi a_0 r_0/k$ this field gives the physical acceleration beyond the Newtonian one felt by test particles in the quasi-Newtonian region.

We learn that the highest fractional correction in this regime is achieved close to ellipsoid (38) and is of order $k/(4\pi)$, around a 0.0025 for $k \approx 0.03$; it then falls off as $1/r^2$ as we move away from the SP. Therefore, as long as we do not use (18) for fractional corrections larger than $k/(4\pi)$ we obtain qualitatively correct results (the example given in Sec. III satisfies this condition).

The bottom line for our predictions is that the ellipsoid (38) represents both the region where the largest linear corrections are felt and the border for the onset of full MOND behavior. For the three examples considered in Sec. III we have

$$r_0 \approx 383 \text{ Km} \qquad \text{Earth-Sun,} \qquad (58)$$

$$r_0 \approx 9.65 \times 10^5 \text{ Km} \qquad \text{Jupiter-Sun,} \qquad (59)$$

$$r_0 \approx 140 \text{ Km} \qquad \text{Earth-Moon,} \qquad (60)$$

corresponding to ellipsoids with major semiaxis of 766 Km (Sun-Earth), $1.93 \times 10^6$ Km (Sun-Jupiter), or 280 Km (Earth-Moon). These are the relevant dimensions of the MOND bubbles.

## VI. THE DEEP MOND REGION

By Eq. (28) the deep MOND regime ($\mu \ll 1$) entails $\kappa \approx 4$ or $U \ll 1$. Thus in Eq. (31) we replace $1 + U^2 \to 1$. Then together with Eq. (30) this has a double symmetry, already noticed by Milgrom [15]. They are both invariant under $\mathbf{U} \to \text{const.} \times \mathbf{U}$ (rescaling), and under $\mathbf{x} \to \lambda\mathbf{x}$ (di-

lation of the coordinates). The first symmetry implies that the normalization of $\mathbf{U}$ is arbitrary (of course the normalization is eventually fixed by taking cognizance of the sources of Eq. (30)). The second means that a solution whose linear scale is expanded remains a solution.

In spherical polar coordinates Eqs. (30) and (31) take the form

$$\frac{1}{r^2} \frac{\partial}{\partial r}(r^2 U_r) + \frac{1}{r\sin\psi} \frac{\partial}{\partial \psi}(\sin\psi U_\psi) = 0, \qquad (61)$$

$$\left[\frac{4}{r}\left(\frac{\partial(rU_r)}{\partial r} - \frac{\partial U_\psi}{\partial \psi}\right) + \left(\frac{U_r}{r}\frac{\partial}{\partial \psi} - U_\psi \frac{\partial}{\partial r}\right)\right]U^2 = 0. \quad (62)$$

For a solution of these to turn into a second solution upon dilatation of the coordinates ($r \to \lambda r$), it is necessary for the $r$ dependence of both $U_r$ and $U_\psi$ to be a single power. Thus we make the ansatz

$$\mathbf{U} = C\left(\frac{r}{r_0}\right)^{\alpha-2}(F(\psi)\mathbf{e}_r + G(\psi)\mathbf{e}_\psi) \qquad (63)$$

with $C$ and $\alpha$ dimensionless constants. The power $\alpha - 2$ was chosen for notational convenience in what follows. Substituting in Eq. (61) we obtain

$$G' + \text{ctan}(\psi)G + \alpha F = 0 \qquad (64)$$

while substitution in Eq. (62) gives

$$F\frac{d(F^2 + G^2)}{d\psi} + 2[\alpha G - 2F'](F^2 + G^2) = 0. \qquad (65)$$

These last constitute a coupled system of first order ordinary differential equations for $F(\psi)$ and $G(\psi)$.

These equations have several symmetries. $F$ and $G$ may be rescaled, that is multiplied by a constant (this is nothing but the scale-invariance of the deep MOND regime). We also have the symmetry: $\alpha \to -\alpha$, $F \to F$, $G \to -G$. Finally the equations are parity-invariant:

$$\psi \to \pi - \psi, \qquad F \to \pm F, \qquad G \to \mp G. \qquad (66)$$

Of course this by itself does not compel the solutions themselves to have definite parity, i.e. $F(\psi) = \pm F(\pi - \psi)$ and $G(\psi) = \mp G(\pi - \psi)$. However, numerically we find that the only regular solutions are indeed those with definite parity, and that these only exist for a discrete sequence of $\alpha$s: $\{\pm \alpha_1, \pm \alpha_2, \cdots\}$. Specifically we find $\alpha_1 = 2$ and the approximate values $\alpha_2 \approx 3.528$, $\alpha_3 \approx 5.039$, $\alpha_4 \approx 6.545$, etc.

Seen in another way, the boundary conditions at $\psi = 0$ (see below) justify representing $F$ as a Fourier series in $\cos(m\psi)$ and $G$ as a Fourier series in $\sin(m\psi)$. It is only for the mentioned special $\alpha$s that even and odd $m$ modes decouple, so that we can have a solution that is a series in only odd or only even $m$. For other values of $\alpha$ the solutions mix even and odd $m$, but are singular at $\psi = \pi$.

We further found numerically that each of the regular solutions is dominated by a single Fourier mode, i.e. it is of

the form $F \approx F_0 + F_n \cos n\psi$ and $G \approx G_n \sin n\psi$ for a given $n$. The solution corresponding to $n = 1$ is obtained for $|\alpha_1| = 2$ and is exactly $F = a \cos\psi$ and $G = \mp a \sin\psi$ ($a$ is a constant) for $\alpha = \pm 2$, respectively. We have been unable to find analytic expressions for other coefficients $F_n$ and $G_n$, but have determined them numerically. We now select the relevant solution by imposing appropriate boundary conditions for our problem.

As in Sec. V the boundary condition that the normal component of **U** vanishes requires that we take $G(\psi = 0) = G(\psi = \pi) = 0$. Because $C$ can still be adjusted, we lose no generality in requiring the corresponding boundary condition $F(\psi = 0) = F(\psi = \pi) = 1$. For were we to demand $F(\psi = 0) \neq F(\psi = \pi)$, we would thereby introduce a jump in **U** across the plane $\psi = \pi/2$ for which there is no physical reason. Our choice of boundary conditions immediately selects a solution with definite parity, which as mentioned earlier, are the only nonsingular ones. Regarding boundary conditions at large $r$, we know that there must be a match with the field in the quasi-Newtonian region. This naturally selects the particular solution with $n = 2$, since the quasi-Newtonian solution $\mathbf{U}_0$ has components with angular profiles of form $\cos 2\psi$ or $\sin 2\psi$. This logic still does not prefer positive over negative $\alpha$. But to avoid a singularity at the origin (see Eq. (63)) we should select the solution with positive $\alpha$, namely, that for $\alpha \approx 3.528$.

The functions $F$ and $G$ obtained for this $\alpha$ are plotted in Fig. 6. These graphs are approximated at the level of 1% by the formulae

$$F(\psi) = 0.2442 + 0.7246 \cos(2\psi) + 0.0472 \cos(4\psi),$$
$$G(\psi) = -0.8334 \sin(2\psi) - 0.0368 \sin(4\psi). \tag{67}$$

For comparison Fig. 6 plots also $N_r$ and $N_\psi$ of Eqs. (35)–(37). We see that the angular profile of the deep MOND **U** (whose flow is plotted in Fig. 7) is quite similar to that of the Newtonian $\mathbf{U}_0$ (Eq. (40) and Fig. 2). Of course, the radial dependences of the two are quite different. Now as mentioned earlier, in the absence of any mention of the sources in Eqs. (30) and (31), it is not possible to determine the normalization of **U**. However, we may estimate $C$ in Eq. (63) as follows. Given the similarity



FIG. 7. The flow of the field **U** in the deep MOND regime plotted with linear scale in units of $r_0$ and assuming $C = 1$.

of the angular profiles we may suppose that were we to extend the deep MOND **U** of Eq. (63) to the inner boundary of the Newtonian region at $r = r_0$, we should obtain $\mathbf{U}_0$. This requires that $C = 1$ and we adopt this value.

We conclude that taking the curl term into account in the deep MOND regime once again vindicates qualitatively the simplified arguments of Sec. III, but introduces substantial quantitative novelties. Using (32) we find that the extra physical force is now

$$\delta \mathbf{F} \approx -\nabla\phi = \frac{4\pi a_0}{k} \frac{\mathbf{U}}{U^{1/2}}. \tag{68}$$

If we define **D** as the angular profile in the deep MOND regime (which as we have seen is very close to **N**) then
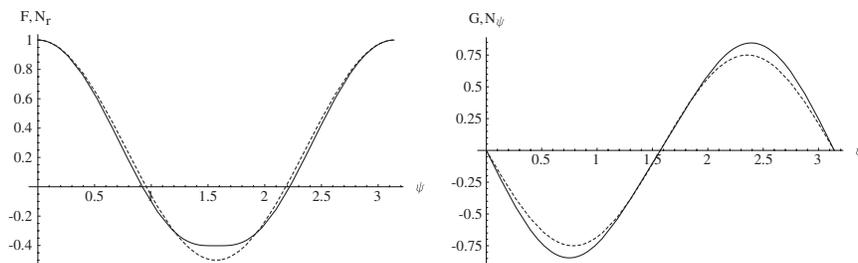


FIG. 6. The numerically determined angular profile functions $F$ and $G$ in the deep MOND region (solid line) compared with the Newtonian profile functions $N_r$ and $N_\psi$ (dotted line), respectively.
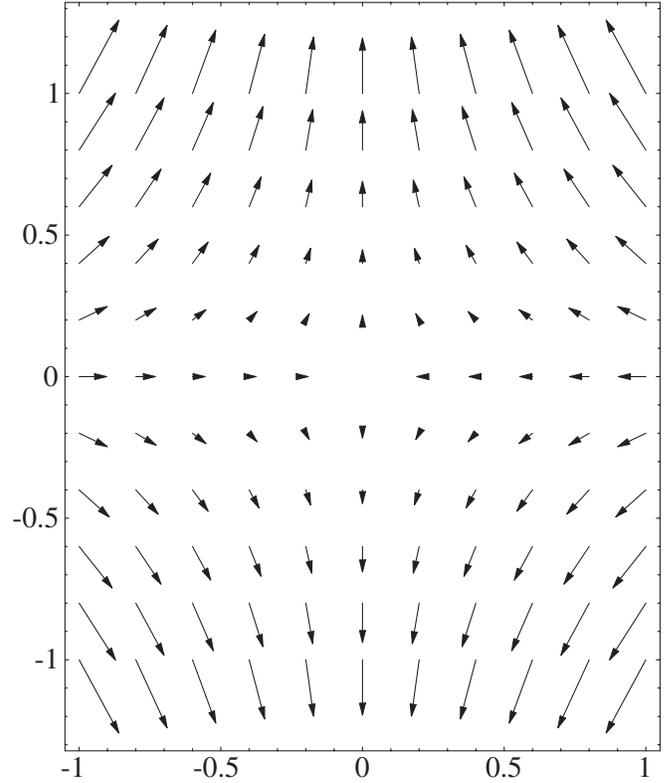
$$\delta \mathbf{F} \approx \frac{4\pi a_0}{k} \left(\frac{r}{r_0}\right)^{(\alpha-2)/2} \frac{\mathbf{D}}{D^{1/2}}. \qquad (69)$$

For $\alpha < 4$ (a condition satisfied by our solution), the tidal stresses associated with this field, i.e. its spatial derivatives, diverge at the saddle, as predicted in Sec. III. However the divergence is softer than in Eq. (16) where the curl term was ignored (that solution corresponds to $\alpha = 3$, which is an unphysical value as we have seen).

Rearranging (69) with the aid of the definition of $r_0$ and Eq. (34) we find that the continuation of formula (57) in the deep MOND regime is

$$\frac{\delta F}{F^{(N)}} \sim \frac{k}{4\pi} \left(\frac{r_0}{r}\right)^{(\alpha-4)/2} \approx \frac{k}{4\pi} \left(\frac{r_0}{r}\right)^{-0.24}. \qquad (70)$$

Hence the fractional correction to Newtonian gravity, which equals $k/(4\pi) \approx 0.0025$ at the ellipsoid (38), continues to grow in the strong MOND regime as we approach the saddle. (Were we to ignore the curl term, in which case $\delta F/F^{(N)} \sim 1/\sqrt{r}$, this growth would be steeper.) One implication of the growth is that the $\phi$ force overtakes $F^{(N)}$ in a much smaller inner region than naively expected (c.f. formula (17)). Specifically $\delta F \approx F^{(N)}$ at

$$r \sim r_0 \left(\frac{k}{4\pi}\right)^{2/(4-\alpha)} = \frac{a_0}{A} \left(\frac{k}{4\pi}\right)^{2(\alpha-3)/(4-\alpha)}. \qquad (71)$$

This is smaller than (17) by a factor of $10^{-6}$, and is essentially microscopic except for the Jupiter-Sun system. The value of $F^{(N)}$ when it becomes subdominant is not $a_0$ as naively expected; it is also smaller by a factor of $10^{-6}$.

In summary, the full analysis reveals that there is a very large region (given by the ellipsoid (38)) inside which full MONDian effects are present. The fractional MONDian corrections to gravity in this region exceed $k/(4\pi)$ and are therefore significant. However the MOND field only dominates the Newtonian field, i.e. the fractional correction becomes larger than unity, in a region far too small to be observable.

## VII. THE REALISTIC SOLAR SYSTEM

The results of Secs. III, V, and VI can be used to show that the SP location for a pair of masses as determined by pure Newtonian gravity ($\mathbf{F}^{(N)} = -\nabla\Phi_N = 0$) coincides with that determined by full TeVeS ($-\nabla(\Phi_N + \phi) = 0$). In the calculations in Sec. VI the origin $r = 0$ is the point where $\nabla\phi = 0$, and the field configuration of $\nabla\phi$, or its surrogate $\mathbf{U}$, in North and South hemispheres are reflections of each other (see Fig. 7). This configuration acts as a boundary condition for $\mathbf{U}$ in the quasi-Newtonian region (treated in Sec. V). Accordingly, we expect not only the magnetic part $\mathbf{U}_2$, but also the $\mathbf{U}_0$, which serves as background for $\mathbf{U}_2$'s Eq. (42), to reflect the mentioned symmetry, and for the null points of both these fields to coincide with that of $\mathbf{U}$ of the deep MOND region. Now as we move outward from the quasi-Newtonian region, $\mathbf{U}$

becomes dominated by $\mathbf{U}_0$ which is the pure Newtonian field. Hence the SP determined by that field (see Sec. III) coincides with that determined by the full MOND field.

The results presented so far are "model calculations," valid under a number of simplifying assumptions not satisfied by the real SS. For example, orbits are elliptic, not circular; the barycenter of the system does not coincide with the center of $M$; we have a many-body problem, not a two-body problem; etc. To leading order these complications do not change the anomalous effects predicted by MOND around SPs or the size of the regions where they are felt. They do complicate the issue of locating "MOND bubbles," but since their centers coincide with the SPs of the Newtonian potential, this is in fact a Newtonian physics problem, independent of MOND dynamics.

For example the SS barycenter is dominated by the Sun-Jupiter pair and lives just outside the solar surface, rotating with a period of approximately 11 years. But even this is a crude approximation: the relative position of the Sun and any planet depends on the configuration of the entire SS, and is chaotic. The same may be said for the location of the SP between the Sun and that planet. However, with empirical inputs and a numerical Newtonian code we can determine the location of the full set of SPs, and even predict where they will be within a few years [16]. Not only are these details in the realm of Newtonian physics, but they do not affect our conclusions on MOND effects around SPs, as long as we anchor our solutions to wherever Newtonian theory predicts the SPs to be. Indeed we only need the result (14) as a boundary condition for our MONDian calculations.

### A. An example: Epicycles and the many-body problem

However, these practical details do affect the planning of experiments, as we now illustrate. Consider the location of the Earth-Sun and Moon-Earth SPs. Ignoring the effect of the Moon, the Earth-Sun SP is predicted to be well inside the Moon's orbit, so we cannot decouple the two systems. This induces dramatic qualitative changes in the location of both SPs.

Let us assume that within the Moon-Earth orbit the Sun's field is uniform (with strength $a_E$) and parallel to the Lunar orbital plane (this may be refined, but does not alter our point). If we consider a frame attached to the unperturbed Moon-Earth SP, with $z$ pointing away from the Earth and $x$ on the orbital plane, then the Newtonian acceleration for points on this plane is

$$\mathbf{F}_N = A(z\mathbf{e}_z - \tfrac{1}{2}x\mathbf{e}_x) - a_E[\cos(\omega t)\mathbf{e}_z - \sin(\omega t)\mathbf{e}_x], \qquad (72)$$

where $A$ is given by Eq. (13) with $m$ the Moon's mass and $M$ the Earth's, $\omega = 2\pi/T$, $T$ the Moon's synodic period, and $t = 0$ the time when the Sun, Earth, and Moon are aligned (in that sequence). Thus, within these approximations, the actual SP (defined by $\mathbf{F}_N = 0$) describes a

monthly ellipse centered on the unperturbed SP location, with equation

$$x = 2\frac{a_E}{A}\sin(\omega t),  \qquad (73)$$

$$z = \frac{a_E}{A}\cos(\omega t).  \qquad (74)$$

Thus the semimajor axis is $2a_E/A \approx 6.0 \times 10^4$ Km while the semiminor one is $a_E/A \approx 3.0 \times 10^4$ Km; these axes perform an annual rotation so that the smaller axis stays aligned with the Sun. Since the rough prediction (ignoring the Sun) places the SP about $4.3 \times 10^4$ Km away from the Moon, we cannot ignore the details arising from the three-body problem. When all effects are taken into account, the SP may encounter the Moon's surface in its motion.

Other perturbations superpose further ellipses upon this motion, each aligned with the direction of its source. In general the motion of the SP is a series of elliptic epicycles of this form due to all possible perturbations on the main two-body system.

It should be pointed out that the fact that the Earth-Moon system falls freely in the field of the Sun does not alter the above arguments (see Appendix). In spite of the weak equivalence principle, the criterion for strong MOND effects is that the field $\mathbf{F}^{(N)}$ calculated in the global frame becomes comparable to $a_0$ so that $\nabla\phi$ can make a significant and identifiable contribution to the overall gravitational field $-\nabla(\Phi_N + \phi)$. Hence the position of the SP is to be determined, to first order, as done above.

### B. MOND bubbles as accelerometers

There is a fine detail of the SP system that is purely MONDian: sensitivity to the extra-solar potential, or more precisely, to the peculiar acceleration, $a_p$, of the SS barycenter. As explained before, MONDian behavior can only be identified from the total potential and this *must* include the extra-SS component. In Newtonian theory the effect of $a_p$ passes unnoticed because nothing dramatic distinguishes the SP; by contrast in MOND the SP is signaled by diverging tidal forces. The fact that we are free-falling in this field is irrelevant as just mentioned. We note that $a_p$ does not shift the location of the Lagrange points because their definition involves balancing inertial forces and gravitational fields. Since we are free-falling in the extra-galactic field, aside from making a tidal distortion, this acceleration does not affect the Lagrange points.

The effect of $a_p$ is to superpose a further elliptical motion onto the larger epicycles due to intrasolar perturbations. If $\mathbf{a}_p = \{a_{pz}, a_{px}, a_{py}\}$ in the system of axes used above, then a similar calculation leads to

$$z = \frac{2}{A}(a_{pz}\cos(\omega' t) - a_{px}\sin(\omega' t)),  \qquad (75)$$

$$x = \frac{2}{A}(a_{pz}\sin(\omega' t) + a_{px}\cos(\omega' t)),  \qquad (76)$$

$$y = \frac{2}{A}a_{py},  \qquad (77)$$

where $\omega'$ is $2\pi$ divided by the Moon's *sidereal* period. We see that the SP is raised off the orbital plane by $a_{py}/A$, and describes an ellipse oriented with $\mathbf{a}_p$ on this plane.

How can we estimate $\mathbf{a}_p$? This is the "acceleration counterpart" to the cosmic microwave background (CMB) dipole (which measures the peculiar velocity $\mathbf{v}_p$ with respect to the cosmological frame). There is no simple way to estimate $\mathbf{a}_p$ other than identifying all components making up $\mathbf{v}_p$ and inferring the acceleration on a case by case basis. Part of $\mathbf{v}_p$ is due to our motion around the Milky Way at 217 Km/s and a radius $r$ of about 26 000 ly. From these figures we infer

$$a = v^2/r \approx 1.9 \times 10^{-10} \text{ m s}^{-2},  \qquad (78)$$

which is comparable to $a_0$. In addition there are "non-linear" peculiar velocity components, such as the movement of the Milky Way about the center of the local group and the motion of the local group toward the great attractor. These are of the order 100–200 Km s$^{-1}$, and deriving their associated acceleration is complex.

When all these nonlinear components are added, the total points in the opposite direction to the CMB dipole (which implies a speed of roughly 300 Km s$^{-1}$), so we may conclude that the peculiar velocity is about 600 Km s$^{-1}$ roughly in the direction of the CMB dipole. In cosmological linear perturbation theory there is a simple relation between peculiar velocity and acceleration, namely

$$a_p = \frac{3}{2}\Omega_m^{0.4} H_0 v_p,  \qquad (79)$$

where $H_0$ is the Hubble constant and $\Omega_m$ is the ratio between the matter density $\rho_m$ and the critical density $\rho_c$ [17]. For currently popular values of these parameters we have $a_p \approx 1.3 \times 10^{-12}$ m s$^{-2}$. (Naively this places velocity perturbations in the MOND regime, but the criterion for MONDian behavior on cosmological scales should be derived from a MONDian counterpart of the above mentioned perturbation theory; this is just now becoming possible [18].)

We may guess that (79) provides a good order of magnitude estimate for the acceleration due to both linear and nonlinear large-scale perturbations. This suggests that the SS peculiar acceleration is dominated by its motion around the center of the galaxy. However, one cannot discount the possibility that the SS has a significant mass in its neighborhood, e.g. undiscovered massive planets or even a stellar companion. This would contribute to $a_p$. In any case, this effect has been constrained using timing data on accurate astronomical clocks [19], leading to the bound $a_p < 5 \times 10^{-11}$ m s$^{-2}$.

The shift of the SP due to $\mathbf{a}_p$ is small, on the order of meters for the Earth-Sun system. But should MONDian behavior as predicted in this paper be discovered, the motion described by the SPs provides our best chance for a *direct* measurement of the peculiar acceleration; MOND bubbles would then function as sensitive accelerometers.

## VIII. TARGETS FOR LISA PATHFINDER

As stated in the introduction, the MOND effects near the Lagrange points are expected to be weak; however this does not mean that they are beyond the reach of very sensitive equipment, such as that on board of the LISA Pathfinder (LPF) mission [12]. Furthermore, while in transit to L1, the satellite may pass close enough to the SP to probe the quasi-Newtonian region examined in Sec. V (the extreme MONDian region described in Sec. VI probably requires a dedicated mission). In the LPF mission two proof masses are suitably shielded from radiation pressure and other annoyances that prevent testing gravitational physics to $a_0$ accuracy in the inner parts of the Solar system. Naturally the satellite itself has to bear radiation pressure, but its orbit is corrected by tracking the free-falling proof masses contained in its inside. The sensitivity to tidal stresses has been quoted as $10^{-15}$ s$^{-2}$ (see [12]).

According to Eq. (13), tidal stresses at the Sun-Earth SP are of the order $A \approx 4.57 \times 10^{-11}$ s$^{-2}$, 4 orders of magnitude larger than LPF's sensitivity. The fractional corrections to Newtonian gravity contained in Eqs. (55) and (56), and plotted in Fig. 5, have a rough order of magnitude given by (57). The tidal stress corresponding to $\delta F$ is thus of order $10^{-13}(r_0/r)^2$ s$^{-2}$ for the illustrative value $k = 0.03$ used in this paper. Therefore LPF would be sensitive to these MONDian corrections if it got to within $10r_0 \approx 3830$ Km of the saddle. This is not overly demanding; the region is the size of a planet. The MOND effects may be even apparent while LPF is in transit to L1.

In contrast, the MONDian tidal stresses felt near L1 are far too small to be at reach of this mission. If $r_L$ denotes L1's distance from the Sun, L1 lies at $R - r_L \approx 1.5 \times 10^6$ Km from Earth; the saddle of the Sun-Earth potential is at $R - r_s \approx 2.6 \times 10^5$ Km from Earth (see Eq. (11)). Therefore L1 is $\Delta r = r_s - r_L \approx 1.24 \times 10^6$ Km away from the saddle, implying suppression of corrections to Newtonian gravity by a factor $\frac{k}{4\pi} \times \frac{(r_0)^2}{\Delta r} \approx 2.4 \times 10^{-10}$. By way of contrast, the Newtonian tidal stresses at L1 are, say for the radial component,

$$\frac{\partial F_r^{(N)}}{\partial r} \approx 8\omega_E^2 \approx 3.17 \times 10^{-13} \text{ s}^{-2} \quad (80)$$

with $\omega_E$ being the angular frequency of the Earth's orbit. This is only 2 orders of magnitude above experimental sensitivity, and so the MONDian corrections to stresses in the vicinity of L1 are 8 orders of magnitude too small for the quoted instrumental sensitivity.

However, "indirect" effects may possibly be detectable by LPF: effects not on its accelerometers but on its path (this comment may apply to other L1 missions). Indeed MOND introduces a small shift to the location of L1 and its surrounding orbits. Combining Eqs. (49), (55), and (56), we obtain an extra acceleration at L1 with radial component of signed magnitude

$$\delta F = \frac{4\pi}{k} \frac{r_0}{\Delta r}\left[\frac{1}{2} - \frac{\pi}{3\sqrt{3}}\right]a_0 \approx -1.3 \times 10^{-12} \text{ m s}^{-2}.$$

$$(81)$$

Hence this extra acceleration predicted by MOND points towards the SP, i.e. away from the Sun and toward the Earth. In the usual calculation, the centrifugal acceleration at L1 is exactly balanced by the gravitational one $F^{(N)}$. This last has absolute magnitude $\omega_E^2 r_L$ and points away from the Sun; thus $F^{(N)}$ has to point towards it. This is why L1 is closer to the Sun than the SP of the potential. With the extra force (81) to balance, L1 is further shifted toward the Sun. In view of Eq. (80), the predicted shift is approximately 4 m.

There is a similar order of magnitude effect on the *orbits* about L1, and while this is not the primary purpose of the LPF mission, we suggest that a careful monitoring of the spacecraft trajectory may be of interest to gravitational physics.

## IX. CONCLUSIONS

Postulating dark matter or MONDifying the gravitational interaction are conceptually conflicting ways of dealing with several anomalous astrophysical observations. While it is possible that these anomalies will themselves decide between the two approaches, a "direct detection" would be far more convincing, for example, ongoing dark matter searches finding a particle with suitable cosmological and astrophysical features [20]. In this paper we examined what might constitute "direct" detection of MOND behavior. We predicted the existence of regions displaying full MOND behavior well inside the Solar system, specifically in bubbles surrounding the saddle points of the gravitational potential. If abnormally high tidal stresses are observed in these regions this would prove MOND beyond reasonable doubt.

How general are our predictions? MOND's solid requirement is that $\tilde{\mu}(x)$ must approach 1 as $x \gg 1$ and $x$ as $x \ll 1$; the interpolating regime between these two asymptotic requirements is far less constrained. In the present work this intermediate regime translates into the quasi-Newtonian calculations presented in Sec. V. For these we chose a reasonable form for $\mu(x)$, Eq. (24), but we should stress that the details are model dependent. For instance, in (18) the leading correction could have been

quartic in $a_0/F$ instead of quadratic, resulting in a different power in the denominator of (42). The extra force $\delta\mathbf{F}$ would then fall off more steeply with $r$.

Accordingly, our calculations in the quasi-Newtonian domain are simply illustrative. We defer to a future publication a thorough study of the effect of the choice of $\mu$ (as dictated by theoretical requirements and extant observations) on planetary orbits [21], Lagrange points, and the Pioneer anomaly [9]. By contrast our predictions for the interior of the ellipsoid (38), as presented in Sec. VI, are robust predictions of the MOND scenario, and of wider validity.

We thus face a dilemma. The strongest MOND effect and the theoretically more robust prediction is that made in Sec. VI for the interior of the ellipsoid (38). However locating it in space may be taxing, particularly since this bubble is noninertial. In contrast, the quasi-Newtonian predictions, e.g. what LISA Pathfinder might find in the vicinity of L1, are geographically less demanding, but the predicted effects are weaker and theoretically less discriminative. Thus observing what we predicted in Sec. V would support the specific model (24) there; however failure to observe it would hardly disprove MOND in general. The interior of the ellipsoid (38) is therefore the prime experimental target for a conclusive test. But one should not despair: systems other than those examined here may naturally reveal the inner core derived in Sec. VI. For example the movement of the saddle point through a diffuse medium—say the rings of Saturn—could be observable.

On a technical note, our calculations once more underline the limitations of the usual folklore that MOND can be obtained by "taking the square root of the Newtonian field when $\nabla\Phi \ll a_0$." This is only true under strict spherical symmetry; in general one must add to the Newtonian field a curl term, which acts as a sort of magnetic gravitational field. As we have seen in the study of saddles, this field cannot be neglected even in the quasi-Newtonian region; and in the deep MOND region neglect of the curl component introduces downright errors in the quantitative details.

There are other regions in the solar system where gradients of the Newtonian potential will be low, e.g. at the center of near-spherical objects. However these are obviously inaccessible. By focusing on the saddle points of the gravitational potential in the solar system we believe we have exposed the best candidates for a direct detection of strong MONDian behavior in our own backyard.

## APPENDIX: THE VIEW INSIDE THE SPACE CAPSULE

The form of the field $\phi$ due to the Sun and Earth as discussed in previous sections is relevant for computing the orbit of a spacecraft or the effects of tidal stresses on experiments within it. Other questions are germane if we are interested in gravitational fields created by the spacecraft's components, as in a space reenactment of the Cavendish experiment. These are the subject of the present section.

As long as the spacecraft's propulsion is off, it will move on a geodesic of the physical metric $\tilde{g}_{\alpha\beta}$ of TeVeS basically because the energy-momentum tensor of matter is conserved with respect to that metric. If we ignore relativistic corrections, this path corresponds to a Newtonian trajectory in the potential $\Phi_N + \phi$ created by the SS. What we wish to ask is, in such an orbit what fields and forces exist within the spacecraft?

If we proceed by analogy with general relativity, one might guess that in the spacecraft's frame of reference the sum of the perturbations $\delta\Phi_N$ and $\delta\phi$ to $\Phi_N$ and $\phi$, respectively, sourced by the spacecraft's structures and free proof masses would constitute the effective gravitational potential determining relative accelerations, etc. Below we show that this is so to sufficient approximation. In effect this result shows that TeVeS complies with the weak equivalence principle (in a freely falling frame external gravity is cancelled out). TeVeS does *not* obey the strong equivalence principle.

In TeVeS the physical metric $\tilde{g}_{\alpha\beta}$ and Einstein metric $g_{\alpha\beta}$ are related by (our signature is $\{-, +, +, +\}$)

$$\tilde{g}_{\alpha\beta} = e^{-2\phi} g_{\alpha\beta} - 2\mathfrak{U}_\alpha \mathfrak{U}_\beta \sinh(2\phi), \qquad \text{(A1)}$$

where $\mathfrak{U}_\alpha$ is the eponymous vector field of the theory; it obeys $g_{\alpha\beta}\mathfrak{U}^\alpha\mathfrak{U}^\beta = -1$. Let $g_{\alpha\beta}$ and $\tilde{g}_{\alpha\beta}$ represent the metrics generated by the SS. In the frame of the freely moving spacecraft (supposed to be nonrotating) the physical metric induced by the SS will be of Minkowski form. The transition from the global frame to the spacecraft frame is effected by projecting the said metrics with the help of a suitable tetrad; its explicit form will not be needed here. We use indices $a, b, c, \cdots$ to label spacecraft frame vectors and tensors.

Now $\phi$ of the SS is small; we regard its value within the spacecraft as a fixed number $\phi^{(0)}$. Likewise, $\mathfrak{U}_a$ in the SS is a unit vector which points solely in the time direction (if we ignore the motion of the SS itself with respect to the Galaxy, etc.). We thus regard $\mathfrak{U}_a$ within the spacecraft as a fixed vector, $\mathfrak{U}_a^{(0)}$, which in general has small space components of order of the craft's velocity. We thus have for the Einstein metric within the spacecraft, to first order in $\phi_0$ and the spatial components of $\mathfrak{U}_a^{(0)}$,

$$g_{ab} = \eta_{ab} + 2\phi^{(0)}\eta_{ab} + 4\phi^{(0)}\mathfrak{U}_a^{(0)}\mathfrak{U}_b^{(0)} + h_{ab}. \qquad \text{(A2)}$$

The final term is the perturbation to the Einstein metric from the energy-momentum tensor of spacecraft components. Within the spacecraft $h_{ab}$ is the only part of $g_{ab}$ whose space variation is significant.

The $g_{ab}$ metric comes from Einstein equations, as modified in T$e$V$e$S [4]; here we work in linear approximation. As is well known, the Einstein tensor can be linearized in terms of second derivatives of the perturbation to $\eta_{ab}$; only $h_{ab}$ enters into it, in the form customary from general relativity, because the rest of the terms are here regarded as constant. Further, here as elsewhere, any raising of indices can be done with $\eta^{ab}$ since the difference between it and $g^{ab}$ is already of first order in small quantities. The sources of the modified Einstein equations contain scalar, vector, and matter contributions. Most are quadratic in $\phi$ and $\mathfrak{U}_a$ derivatives, and thus quadratic in the small $\delta\phi$ and $\delta\mathfrak{U}_a$ corrections to $\phi^{(0)}$ and $\mathfrak{U}_a$ produced by the spacecraft. We can thus ignore these energy-momentum contributions. Some further inspection reveals that two other contributions, that related to the T$e$V$e$S Lagrange multiplier $\lambda$, and that coming from the free function $F$, are likewise negligible.

We conclude that the only source of $h_{ab}$ is the matter of the spacecraft. In T$e$V$e$S apart from the usual source $T_{ab}$ there is one of form $T_{ab}(1 - e^{4\phi})$. Obviously because of the smallness of $\phi$ this last is negligible. The linearized Einstein equations thus look like those in general relativity, and the relevant solutions for $h_{ab}$ are the familiar ones. In particular, the temporal-temporal component is $h_{tt} = -2\delta\Phi_N$. We compute the physical metric in the spacecraft's frame by substituting Eq. (A2) into Eq. (A1) and setting $e^{-2\phi} = 1 - 2(\phi^{(0)} + \delta\phi) + \cdots$, $\sin(2\phi) = 2(\phi^{(0)} + \delta\phi) + \cdots$, and $\mathfrak{U}_a = \mathfrak{U}_a^{(0)} + \delta\mathfrak{U}_a$. We get

$$\tilde{g}_{ab} = \eta_{ab} + h_{ab} - 2\delta\phi(\eta_{ab} + 2\mathfrak{U}_a^{(0)}\mathfrak{U}_b^{(0)}) + \cdots, \quad (A3)$$

where the terms omitted are of second order in the small quantities $\delta\phi$, $\delta\mathfrak{U}_a$, and $h_{ab}$.

In calculating $\tilde{g}_{tt}$ we take note of the fact that $\mathfrak{U}_t^{(0)}$ differs from unity by a term of order of the square of the spacecraft's velocity, which is of the same order as $\Phi_N$. Such a correction is negligible in Eq. (A3). We thus get $\tilde{g}_{tt} = -1 - 2(\delta\Phi_N + \delta\phi)$. Accordingly, in the spacecraft's frame the physical gravitational potential equals $\delta\Phi_N + \delta\phi$ as surmised earlier.

Now we know that $\delta\Phi_N$ comes from Poisson's equation. But how is $\delta\phi$ to be calculated? Let us substitute $\phi = \phi^{(0)} + \delta\phi$ in the scalar equation (3). In the present calculations we shall take cognizance of the spatial gradient of $\phi^{(0)}$ and regard it as large compared to $\nabla\delta\phi$. Linearizing the equation in derivatives of $\delta\phi$ leads to

$$\Delta\delta\phi + 2\xi H^i H^j \partial^2\delta\phi/\partial x^i \partial x^j + \cdots = kG\tilde{\rho}, \quad (A4)$$

$$\mathbf{H} \equiv (|\nabla\phi^{(0)}|^2)^{-1/2}\nabla\phi^{(0)}, \quad (A5)$$

$$\xi \equiv d\ln\mu(Y)/\ln Y, \quad (A6)$$

where $\Delta$ represents the Laplacian and $Y \equiv kl^2|\nabla\phi^{(0)}|^2$. In Eq. (A4) the ellipsis denotes terms with first derivatives of $\delta\phi$ only. Quite in analogy with the eikonal approximation we shall ignore these last; presumably the spacecraft's small scale makes contributions containing only a first derivative of a varying quantity subdominant.

It should be evident that the unit vector $\mathbf{H}$ is antiparallel to the $\mathbf{U}$ (discussed in Secs. II, III, IV, V, and VI) coming from the SS. Aligning the coordinate system in the spacecraft's frame with its $x$ axis in the $\mathbf{H}$ direction (possible at a particular position in the orbit), we see that Eq. (A4) is just a Poisson equation whose $x$ coordinate has been rescaled to $x(1 + 2\xi)^{-1/2}$. Now for our model (24) of $\mu(Y)$ we calculate

$$\xi = \frac{1}{2}\frac{1 - \mu^4}{1 + \mu^4}. \quad (A7)$$

It follows that when the spacecraft is in the deep MOND region ($\mu$ built with $\nabla\phi^{(0)}$ is small compared to unity), we find the $x$ direction is compressed by a factor 2. This is a facet of the "external field effect" [3] whereby MOND effects in a weak field systems are traded for quasi-Newtonian behavior but with rescaling in one direction.

By contrast, with the spacecraft deep in the quasi-Newtonian regime ($\mu \approx 1$), $\delta\phi$ is determined by the usual Poisson equation. With $\delta\phi$ proportional to $\delta\Phi_N$ we only have a (small) rescaling of the effective gravitational constant, or equivalently of Milgrom's $\tilde{\mu}$, a point which has already been mentioned in Sec. II. Thus in a quasi-Newtonian environment, even the superweak fields originating in the spacecraft components behave in everyday (Newtonian) fashion.

[1] M. Milgrom, Astrophys. J. **270**, 365 (1983); **270**, 371 (1983); **270**, 384 (1983).
[2] R. H. Sanders and S. S. McGaugh, Annu. Rev. Astron. Astrophys. **40**, 263 (2002).
[3] J. D. Bekenstein and M. Milgrom, Astrophys. J. **286**, 7

(1984).
[4] J. Bekenstein, Phys. Rev. D **70**, 083509 (2004); **71**, 069901(E) (2005).
[5] R. H. Sanders, Mon. Not. R. Astron. Soc. **363**, 459 (2005).
[6] R. H. Sanders, astro-ph/0601431.

[7] J. M. Romero and A. Zamora, Phys. Rev. D **73**, 027301 (2006); W. F. Kao, astro-ph/0512535; I. Navarro and K. v. Akoleyen, gr-qc/0512109; J. G. Hartnett, astro-ph/0511756; J. W. Moffat, J. Cosmol. Astropart. Phys. 05 (2005) 003; J. R. Brownstein and J. W. Moffat, Astrophys. J. **636**, 721 (2006); Mon. Not. R. Astron. Soc. **367**, 527 ( 2006); A. A. Deriglazov, hep-th/0510015; V. V. Kiselev, gr-qc/0507126; J. P. Mbelek, gr-qc/0402088.

[8] J. D. Bekenstein, in *Second Canadian Conference on General Relativity and Relativistic Astrophysics*, edited by A. Coley, C. Dyer, and T. Tupper (World Scientific, Singapore, 1988), p. 487.

[9] J. Anderson *et al.*, Phys. Rev. Lett. **81**, 2858 (1998); Phys. Rev. D **65**, 082004 (2002).

[10] A. Hellemans, *A Force to Reckon With* (Scientific, Princeton, NJ, 2005), p. 12.

[11] J. R. Brownstein and J. W. Moffat, Classical Quantum Gravity **23**, 3427 (2006).

[12] S. Anza *et al.*, Classical Quantum Gravity **22**, S125 2005; A. Lobo *et al.*, gr-qc/0601096.

[13] M. Milgrom, Astrophys. J. **302**, 617 (1986).

[14] H. S. Zhao and B. Famaey, Astrophys. J. **638**, L9 (2006).

[15] M. Milgrom, Phys. Rev. E **56**, 1148 (1997).

[16] See e.g. http://www.boulder.swri.edu/ hal/swift.html.

[17] J. Peebles, *The Large Scale Structure of the Universe* (Princeton University, Princeton, NJ, 1980).

[18] C. Skordis, astro-ph/0511591.

[19] N. Zakamska and S. Tremaine, astro-ph/0506548.

[20] L. Baudis, astro-ph/0511805; in *Proceedings of the XXII Texas Symposium on Relativistic Astrophysics, Stanford University, 2004*, econf C041213, 0046 (2004).

[21] C. Talmadge *et al.*, Phys. Rev. Lett. **61**, 1159 (1988).